



## Development of normalized soil area index for urban studies using remote sensing data

Akib Javed<sup>1</sup>, Zhenfeng Shao<sup>1</sup>, Bin Bai<sup>2</sup>, Zhuoyang Yu<sup>2</sup>, Jiabing Wang<sup>2</sup>,  
Iffat Ara<sup>3,4</sup>, Md. Enamul Huq<sup>5</sup>, Md. Yeamin Ali<sup>6</sup>, Nayyer Saleem<sup>1</sup>,  
Muhammad Nasar Ahmad<sup>1</sup>, Neema Simon Sumari<sup>7</sup> and Mardia<sup>8</sup>

<sup>1</sup>State Key Laboratory of Information Engineering in Surveying, Mapping and Remote Sensing, Wuhan University, Wuhan, China

<sup>2</sup>Software R&D Center, Kunming Antai Software Co., LTD. Kunming, China

<sup>3</sup>Geography and Environment, Islamic University, Kushtia, Bangladesh

<sup>4</sup>Department of International Politics, Shandong University, Jinan, China

<sup>5</sup>College of Environmental Science, Hohai University, Nanjing, China

<sup>6</sup>Caritas Bangladesh, Bandarban, Bangladesh

<sup>7</sup>Department of Informatics & Information Technology, Sokoine University of Agriculture, Morogoro, Tanzania

<sup>8</sup>Geography and Environmental Studies, University of Rajshahi, Rajshahi, Bangladesh

*Received 16 December 2021, in final form 15 December 2022*

This paper presents two novel spectral soil area indices to identify bare soil area and distinguish it more accurately from the urban impervious surface area (ISA). This study designs these indices based on medium spatial resolution remote sensing data from Landsat 8 OLI dataset. Extracting bare soil or urban ISA is more challenging than extracting water bodies or vegetation in multi-spectral Remote Sensing (RS). Bare soil and the urban ISA area often were mixed because of their spectral similarity in multispectral sensors. This study proposes Normalized Soil Area Index 1 (NSAI1) and Normalized Soil Area Index 2 (NSAI2) using typical multispectral bands. Experiments show that these two indices have an overall accuracy of around 90%. The spectral similarity index (SDI) shows these two indices have higher separability between soil area and ISA than previous indices. The result shows that percentile thresholds can effectively classify bare soil areas from the background. The combined use of both indices measured the soil area of the study area over 71 km<sup>2</sup>. Most importantly, proposed soil indices can refine urban ISA measurement accuracy in spatiotemporal studies.

*Keywords:* soil index, NSAI1, NSAI2, LULCC, Dhaka

## 1. Introduction

Spectral confusion among soil area and impervious surface area (ISA) is a major classification problem in optical remote sensing (RS) which affects both soil and urban-related studies (Waqar et al., 2012). Soil indexing is important for mapping global barren land, sandy areas, land use land cover (LULC) studies, forest health monitoring, agricultural activities, geological crust, drought-prone area, and so on. More importantly, refinement of soil area indexing has particular application for better urban impervious surface area (ISA) classification. Bare soil and ISA have similar spectral characteristics (Qiu et al., 2017). Therefore, better soil area measurement will assist with more refined urban ISA classification. Bareness Index (BI2014) (Li and Chen, 2014), Normalized Difference Bare Land Index (NBLI) (Li et al., 2017) and Modified Normalized Difference Soil Index (MNDSI) (Piyooosh and Ghosh, 2017) are three such examples.

Earlier, many urban spectral indices, such as normalized difference built-up index (NDBI) (Zha et al., 2003), Urban index (UI) (Kawamura et al., 1997), enhanced built-up and bareness index (EBBI) (As-syakur et al., 2012), index based built-up index (IBI) (Waqar et al., 2012) and NDBI of Bhatti and Tripathi (2014) did not differentiate bare soil areas and urban area. Besides, normalized difference built-up index (NDBI) (Zha et al., 2003) and normalized difference soil index (NDSI) (Rogers and Kearney, 2010) are essentially the same index with different names and purposes. The same index is sometimes used for urban and soil area mapping.

Later, Demattê et al. (2009) examine soil area detection methods from Landsat TM image. This study examines soil colour composite, soil line information using Red-NIR feature space, absence of vegetation index value and comparing the spectral curve characteristics of soil area. In conclusion, the study suggests using spectral patterns and other soil information to detect soil pixel areas for accurate soil classification.

A significant advancement came in separating Urban ISA from soil area with Biophysical Composition Indices (BCI) (Deng and Wu, 2012). It can extract urban ISA while suppressing bare soil signature using tasseled cap transformed (TCT) bands. However, the separability of bare soil and ISA using BCI is mild. Besides BCI, modified normalized difference soil index (MNDSI) (Hua et al., 2017), ratio normalized difference soil index (RNDSI) (Deng et al., 2015) are a few significant studies that dealt with spectral confusion of soil areas and ISA.

Although Modified Normalized Difference Soil Index (MNDSI) separates bright soil areas using Panchromatic (PAN) bands quite efficiently, the PAN band is a recent addendum and unavailable among all Landsat missions. Furthermore, Landsat ETM+ and Landsat OLI have different spectral ranges for the PAN band. Therefore, any temporal studies beyond Landsat 7 ETM+ will not be feasible with PAN bands. The same issue prohibits us from using thermal and coastal bands too.

The soil had higher reflectivity in all the infrared multispectral bands than visible bands, especially in the SWIR1 spectral region than the NIR wavelength region. Based on that, Rogers and Kearney (2010) introduced a soil index named Normalized Difference Soil Index (NDSI). Similarly, soil shows slightly higher reflectivity in the thermal region than the SWIR1 region, used in the normalized difference bareness index (NDBaI) (Zhao and Chen, 2005). NDBaI also utilizes thermal (TIR) bands since the soil area reflects higher in the TIR spectral region. Similarly, Waqar et al. (2012) proposed a new soil index (SI) using a TIR band and SWIR2 band from Landsat TM and claimed that SI increases the soil extraction accuracy by 11% more than all previous soil indices. Later, Li et al. (2017) proposed Normalized Difference Bare Land Index (NBLI) using TIR and Red bands. This study is also significant because they aim to classify urban LULC classes with NBLI. This study claims that it got closer to supervised SVM classification results and applied in temporal applications too. However, their soil mapping is too poor and works best with bright soil areas.

In addition, BCI, TCT bands are also used in RNDSI (Deng et al., 2015). In TCT, the first band is dedicated to brightness or whiteness. It is attributed to bright land features, soil, white bare land, sands etc. It is often called TC1, TCB or brightness (Baig et al., 2014). More importantly, TCT coefficients have been developed for all the major multispectral sensors making TCT bands compatible with multi-sensorial studies. On the other hand, soil areas are highly heterogeneous in colour and composition. Therefore, any single-colour dependency is unrealistic for the soil area index.

Furthermore, lack of vegetation or absence of greenness is also used in spectral soil area indexing. Such as NDSI<sub>2015</sub>, Modified Bare Soil Index (MBSI) and Biological Soil Crust Index (BSCI); all three of the indices subtract the Green bands in their indices (Chen et al., 2005; Deng et al., 2015; Zhang et al., 2018). Additionally, the NIR band, which is highly sensitive to chlorophyll, is subtracted from Normalized Difference Soil Index (NDSI<sub>2010</sub>) and Bare Soil Index (BI<sub>2002</sub>) (Rikimaru et al., 2002; Rogers and Kearney, 2010). More distinctly, in DBSI, NDVI is also subtracted after the Green band has been subtracted from SWIR1 (Rasul et al., 2018). Similarly, the second TCT band or greenness is used in deduction to formulate BCI (Deng and Wu, 2012). On the contrary, the Partially Normalized Sandy Barren Index (PNSBI) took the opposite approach and the Coastal band was deducted from the Green band (Zhao et al., 2019).

Wetness or soil moisture is also sensitive and highly absorbent of all the infrared multispectral bands. But soil indices are highly dependent on infrared bands such as NIR, SWIR1 & SWIR2. Dry soil and wet soil are indexed differently due to this sensitivity. Any moisture or water particles in air or soil significantly influence soil indexing outcome. Therefore, the RS image's season and time are also considered for better soil indexing results. Similarly, the shadow of clouds, mountains and tall buildings also adversely affects soil area indexing.

In microwave remote sensing, soil mapping mostly focuses on soil moisture mapping or sub-surface soil mapping. L-band microwave imaging can penetrate vegetation and is good for soil surface mapping. C-band microwave imaging deals more with atmosphere and weather patterns. X-band microwave imaging can offer higher resolution and more details imaging. Soil characteristics with sand, silt and clay with their moisture content were studied with X-band microwave imaging (Srivastava and Mishra, 2004). Dual frequency radar imaging is also common for soil moisture studies (Balenzano et al., 2013; Prevot et al., 1993; Taconet et al., 1994). In another study, a new method based on Dubois for measuring soil moisture and roughness uses a wide range of incidence angles and radar wavelengths, including L, C, and X bands (Baghdadi et al., 2016). Besides frequency, different type of radar remote sensing has application in soil studies. Such as, synthetic aperture radar (SAR) can provide accurate soil moisture mapping in non-destructive ways (Boisvert et al., 1996). Ground penetrating radar (GPR) is also potent in measuring soil water content (Huisman et al., 2003; Klotzsche et al., 2018; Liu et al., 2019). But, GPR is focused on sub-surface soil studies, such as characterizing soil and peat stratigraphy and detecting tree roots (Zajícová and Chuman, 2019). Advanced synthetic aperture radar (ASAR) can also map soil tillage and moisture (McNairn and Brisco, 2004). Combining optical and microwave remote sensing has potential applications in agricultural soil studies, such as soil tillage and irrigation channels (Hadria et al., 2009). There is a lack of studies on classifying bare soil from the impervious surface area using microwave remote sensing. Although microwave remote sensing is good at measuring some soil characteristics, it cannot generalize soil areas as optical remote sensing do. Optical remote sensing also studies soil moisture or lack of it and can index them.

Lack of moisture, low vegetation, and dried soil is considered drought (Mishra and Singh, 2010). In soil indexing, droughts are essential in measuring the lack of water and vegetation. Ghulam et al. (2006) developed a simple and effective drought monitoring index using the spectral space of NIR and Red band. It is named perpendicular drought index (PDI), which was later upgraded as modified PDI (MPDI) developed to monitor real-time drought by using scaled NDVI (Ghulam et al., 2007). Later, Li and Tan (2013) combined vegetation and water to develop Second Modified Perpendicular Drought Index (MPDI1).

In similar studies,  $BI_{2002}$ ,  $BI_{2014}$ , MBSI, MNDBaI and PNSBI indices are all focused on indexing the bareness or brightness of the soil area. Crust Index (CI) and Biological Soil Crust Index (BSCI) is emphasized in indexing soil crust. All these indices are well-fitted for desert-related studies. Except PNSBI, all these indices use Red spectral bands to deduct from to formulate their indices. CI is important for studying soil characteristics, such as stability, fertility, moisture, soil composition and more. BSCI is also important in the desert context to classify biological soil crust, bare ground, vegetation and dried plant materials.

In this study, our first objective is to develop soil area indices from Landsat imagery with better separability of soil areas and urban ISA; secondly, to make these indices applicable for temporal applications, which means these indices only use frequent multispectral bands from Landsat missions. In addition, for better enhancement of soil areas for soil related studies, these two indices will also help refine urban ISA measurements. Moreover, the indices design is formed so that these indices remain applicable for temporal, multi-sensorial, and large-scale regional studies.

## 2. Materials and methods

In the study of spectral soil indexing, various keywords are used within the optical RS domain, such as bare soil areas, bare soil, bare land, barren lands, sandy barren land, bareness index, dryness index, drought index, soil crusts, crust index etc. This study used ‘Soil Area’ or ‘soil’ to refer to all kinds of bare soil and sandy areas.

### 2.1. Study area

Dhaka is a megacity situated in a hot and humid tropical climate (Fig. 1). The city has an annual mean temperature of 25.5 °C (Yamane et al., 2014), average annual precipitation of 2148 mm, and average humidity of 75%. It has a history of remaining the region’s capital for its strategically secure location surrounded by water bodies, rivers and wetlands. Many water bodies are disappear-

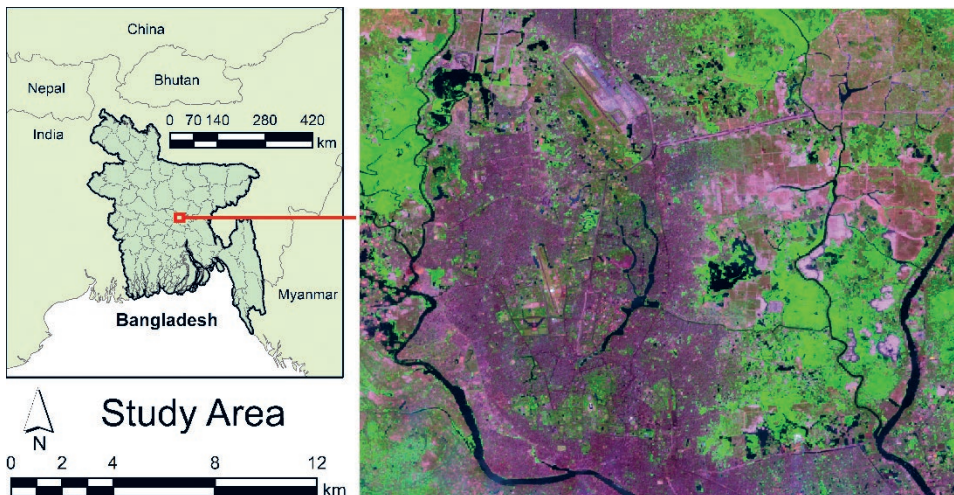


**Figure 1.** Study area of Dhaka city in false colour composition using SWIR1, NIR and Green multispectral bands from Landsat OLI. The light pink colour indicates the presence of soil area, magenta is ISA, green is vegetation, and black is water.

ing in recent encroachments because the sand filling of wetlands and river encroachments reclaim new lands.

Dhaka has shown rapid growth in recent decades. Hence developing newer satellite cities, large landfilled areas, deforestation, and surrounding river and water bodies has made Dhaka city a good case study for the urban soil area index.

## 2.2. Data source

The study uses Google Earth Engine (GEE) for data preparation, index formulation, measuring soil area, extracting indexed comparison maps and so on. The study also used google earth imagery for its higher spatial resolution during accuracy assessment. The study used USGS Landsat 8 level 2, Collection 2, Tier 1 dataset. It is a surface reflectance product of Landsat 8 and has been atmospherically corrected by the GEE team.

All the spectral bands are stored in 16-bit information. It is apparent that unlike USGS Landsat 8 Collection 1 Tier 1 dataset, this dataset does not contain PAN (0.52–0.90  $\mu\text{m}$ ), Cirrus (1.36–1.38  $\mu\text{m}$ ) and thermal band 11 (11.50–12.51  $\mu\text{m}$ ).

Table 1. Spectral bands details of USGS Landsat 8 Level 2, Collection 2, Tier 1.

Band name	Wavelength ( $\mu\text{m}$ )	Description	Name in the text
SR_B1	0.435–0.451	Band 1 (ultra-blue, coastal aerosol) surface reflectance	Coastal
SR_B2	0.452–0.512	Band 2 (blue) surface reflectance	Blue
SR_B3	0.533–0.590	Band 3 (green) surface reflectance	Green
SR_B4	0.636–0.673	Band 4 (red) surface reflectance	Red
SR_B5	0.851–0.879	Band 5 (near infrared) surface reflectance	NIR
SR_B6	1.566–1.651	Band 6 (shortwave infrared 1) surface reflectance	SWIR1
SR_B7	2.107–2.294	Band 7 (shortwave infrared 2) surface reflectance	SWIR2
ST_B10	10.60–11.19	Band 10 surface temperature.	TIR

## 2.3. Construction of NSAI1 and NSAI2

The study proposes two novel soil indices; Normalized Soil Area Index 1 (NSAI1) and Normalized Soil Area Index 2 (NSAI2). NSAI1 normalized the difference between the square of SWIR1 band and the multiplication of Green and NIR bands (Eq. 1). NSAI2 normalized the difference between the multiplication of SWIR1 & Blue bands and the multiplication of Green and NIR bands (Eq. 2).

$$\text{NSAI1} = \frac{\text{SWIR1}^2 - (\text{Green} \times \text{NIR})}{\text{SWIR1}^2 + (\text{Green} \times \text{NIR})} \quad (1)$$

$$\text{NSAI2} = \frac{(\text{SWIR1} \times \text{Blue}) - (\text{Green} \times \text{NIR})}{(\text{SWIR1} \times \text{Blue}) + (\text{Green} \times \text{NIR})} \quad (2)$$

Both of the indices utilize Green, NIR and SWIR1 bands. In NSAI2, additionally, Blue band is used to increase soil sensitivity toward different areas.

The study used only four bands of the pre-processed Landsat 8 surface reflectance image using GEE. All the bands remain unmodified while used in the index's calculation. Later on, the study used one percent trimming from both ends to reduce outliers.

#### 2.4. Related earlier Indices

In Tab. 2, indices have slightly modified their expression to maintain a general representation. All the indices are shown with Landsat missions spectral bands naming style. Additionally, the same acronym differentiates using their respective published year.

Table 2. Description of soil area indices.

Index	Full Name	Expression	Purpose	Classification	Reference	Eq.
NDSI <sub>2010</sub>	Normalized Difference Soil Index	$\frac{\text{SWIR1} - \text{NIR}}{\text{SWIR1} + \text{NIR}}$	Coastal marsh mapping	Simple Soil Index	Rogers and Kearney (2010)	(3)
TC1	Tasseled Cap One or Brightness	$\frac{\text{Blue} * 0.3029 + \text{Green} * 0.2786 + \text{SWIR1} * 0.508 + \text{SWIR2} * 0.1872}{\text{Blue} * 0.3029 + \text{Green} * 0.2786 + \text{SWIR1} * 0.508 + \text{SWIR2} * 0.1872}$	White area mapping	Composite Soil Index	Kauth and Thomas (1976)	(4)
NDSI <sub>2015</sub>	Normalized Difference Soil Index	$\frac{\text{SWIR2} - \text{Green}}{\text{SWIR2} + \text{Green}}$	Soil mapping	Simple Soil Index	Deng et al. (2015)	(5)
RNDSI	Ratio Normalized Difference Soil Index	$\frac{\text{NNDSI}_{2015}}{\text{NTC1}}$ where, NNDSI <sub>2015</sub> is normalized NDSI <sub>2015</sub> and NTC1 is normalized TC1	Improved soil mapping	Composite Soil Index	Deng et al. (2015)	(6)
NDBaI	Normalized Difference Bare-soil Index	$\frac{\text{SWIR1} - \text{TIR}}{\text{SWIR1} + \text{TIR}}$	Soil mapping	Simple Soil Index	Zhao and Chen (2005)	(7)

Table 2. Continued.

Index	Full Name	Expression	Purpose	Classification	Reference	Eq.
BI <sub>2014</sub>	Bareness Index	$\frac{1}{2}(\text{NTC1}, \text{NNDBaI})$ <p>where, NTC1 is normalized TC1 and NNDBaI is normalized NDBaI</p>	Soil index for improving urban mapping	Composite Soil Index	Li and Chen (2014)	(8)
BI <sub>2002</sub>	Bare soil Index	$\frac{(\text{SWIR2} + \text{Red}) - (\text{NIR} + \text{Blue})}{(\text{SWIR2} + \text{Red}) + (\text{NIR} + \text{Blue})}$	Forest bare land mapping	Composite Soil Index	Riki-maru et al. (2002)	(9)
SI	Soil Index	$\frac{\text{TIR} - \text{SWIR2}}{\text{TIR} + \text{SWIR2}}$	Soil mapping	Simple Soil Index	Waqar et al. (2012)	(10)
NBLI	Normalized Difference Bare Land Index	$\frac{\text{Red} - \text{TIR}}{\text{Red} + \text{TIR}}$	Soil mapping	Simple Soil Index	Li et al. (2017)	(11)
MNDSI	Modified Normalized Difference Soil Index	$\frac{\text{SWIR2} - \text{PAN}}{\text{SWIR2} + \text{PAN}}$	Soil index for improving urban mapping	Simple Soil Index	Piyooash and Ghosh (2017)	(12)
DBSI	Dry Bare Soil Index	$\frac{\text{SWIR1} - \text{Green}}{\text{SWIR1} + \text{Green}} - \text{NDVI}$	Drought mapping	Composite Dry Soil Index	Rasul et al. (2018)	(13)
PDI	Perpendicular Drought Index	$\frac{1}{\sqrt{1.4042^2 + 1}}(\text{Red} + 1.40426 * \text{NIR})$	Drought mapping	Simple Dry Soil Index	Ghulam et al. (2006)	(14)
MBSI	Modified Bare Soil Index	$\frac{(\text{Red} - \text{Green}) * 2}{(\text{Red} + \text{Green}) - 2}$	Soil mapping	Simple Soil Index	Zhang et al. (2018)	(15)
PNSB	Partially Normalized Sandy Barren Index	$\frac{\text{Green} - \text{Coastal}}{\text{Green} + \text{Coastal}}$ <p>when, NIR-Red&gt;0</p>	Sand mapping	Simple Dry Soil Index	Zhao et al. (2019)	(16)
CI	Crust Index	$\frac{1 - (\text{Red} - \text{Blue})}{(\text{Red} + \text{Blue})}$	Sand mapping	Simple Dry Soil Index	Karnieli (1997)	(17)
BSCI	Biological Soil Crust Index	$\frac{1 - 2 * (\text{Red} - \text{Green})}{\frac{1}{3} * (\text{Red} + \text{Green} + \text{NIR})}$	Sand mapping	Composite Dry Soil Index	Chen et al. (2005)	(18)
MNDI	Modified Normalized Difference Barren Index	$\frac{\text{Red} - \text{Blue}}{\text{Red} + \text{Blue}}$	Soil index for improving urban mapping	Simple Soil Index	Hua et al. (2017)	(19)

### 2.5. Accuracy assessment

Both of the indices have been tested for a handful of thresholds. But the study presented only two thresholds for each index which are more accurate. For accuracy assessment, randomly selected 500 points were checked against higher resolution google earth images. For higher accuracy, the study used visual interpretation from Google Earth Imagery and threshold-based pixel information of soil area or no soil area in binary from GEE.

The assessment presented NSAI1 with 85%, 87.5% and NSAI2 with 90%, 92.5% percentile threshold. The assessment also shows the combination of NSAI1 with 85% threshold and both NSAI2 thresholds. These threshold applications resulted in a binary image where '1' refers to the soil area, and '0' refers to the non-soil area.

These random points were manually checked with the help of Google Earth image and a natural RGB compilation of raw images. Thus, the accuracies are calculated with the respective formula.

### 2.6. Calculation of Spectral difference index (SDI)

The study used the spectral difference index (SDI) (Radeloff et al., 1999) between urban ISA and soil area to see which indices have the highest value in separating them. This study considers popular soil indices with typical multi-spectral spectral bands and newly proposed soil indices for SDI calculation. SDI provides the positive value of the mean difference of two classes divided by the standard deviation addition of two classes (Eq. 20). In this study, two LULC classes refer to urban ISA and soil classes.

$$SDI = \left| \frac{\bar{\mu}_1 - \bar{\mu}_2}{\bar{\sigma}_1 + \bar{\sigma}_2} \right|, \quad (20)$$

where,  $\bar{\mu}_1$  and  $\bar{\mu}_2$  refers to the mean index value of urban ISA and soil classes, respectively. Similarly,  $\bar{\sigma}_1$  and  $\bar{\sigma}_2$  refers to the standard deviation of urban ISA and soil classes respectively. For SDI calculation, manually digitized sample areas for each LULC classification were used. Google Earth image and Landsat RGB combination were used for digitizing LULC classes.

The BCI is also measured in the SDI calculation with other soil indices. Because, it is a crucial urban index that attempts to suppress soil signature during urban ISA indexing. The study examines how it fits the study area. BCI normalized the mean of TC1 and TC3 values and the TC2 value difference. The index calculation is shown below.

$$BCI = \frac{(H+L)/2 - V}{(H+L)/2 + V}, \quad (21)$$

where H, V and L are normalized forms of TC1, TC2 and TC3 bands (Deng and Wu, 2012). H comes from 'High albedo', V comes from 'Vegetation', and L comes

from ‘Low albedo’. H, V and L have used the normalization function shown (eq.22) below:

$$\text{Normalized TC} = \frac{\text{TC} - \text{TC}_{\text{MIN}}}{\text{TC}_{\text{MAX}} - \text{TC}_{\text{MIN}}} \quad (22)$$

Normalized TC formula made all three TC bands normalized within 0–1. Therefore, the value of BCI also remain within –1 to +1.

### 3. Result

#### 3.1. Soil area of Dhaka city

NSAI1 and NSAI2 effectively enhance soil characteristics from the background. NSAI1 shows more sensitivity towards older reclaimed lands, whereas NSAI2 shows more sensitivity towards newly reclaimed lands. Here, only two combinations of both indices are presented. However, other combinations with different thresholds are also possible.

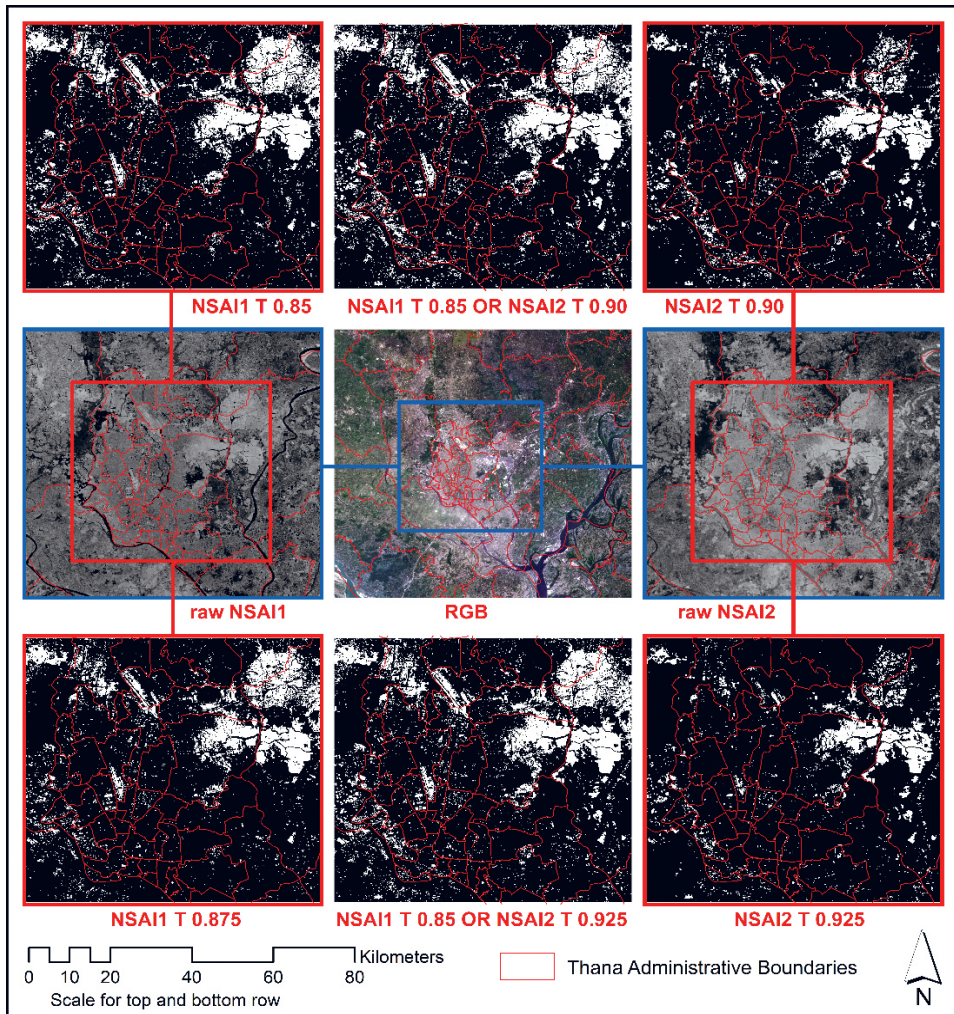
Eastward land reclamation by wetland encroachment is the main reason for Dhaka’s unusual and concentrated soil area. An early study identified the newly reclaimed land as ‘Sub-flood Zone’ (Khaleda et al., 2017). These two indices marked the sand-filled encroached land area in the agglomerated condition. These low-lying wetlands of Eastern Dhaka are almost lost because of landfilling.

Table 3. shows that with each 2.5% threshold change, every index is reduced to more than 10 km<sup>2</sup>. Contrary, instances E and F show more stable results with the same 2.5% changes.

Figure 2 shows that NSAI1 is better sensitive to soil areas that are fellow land, slightly wet and have slight greenness. It also cannot detect very obvious bright sand. In contrast, NSAI2 is better sensitive to brightness, whiteness and newly sand-filled area. Additionally, Soil areas are distinguished from deep water with NSAI1 and shallow water with NSAI2. Combining both indices can bring better results (Fig. 2, E and F).

Table 3. Measurement of soil area for respective indices with specific thresholds.

Instance	Index with threshold	Soil area (km <sup>2</sup> )
A	NSAI1 T 85%	68.36
B	NSAI1 T 87.5%	57.14
C	NSAI2 T 90%	45.10
D	NSAI2 T 92.5%	34.87
E	Combination of A OR C	75.49
F	Combination of A OR D	71.78



**Figure 2.** Extracted soil areas shown in white.

### 3.2. Indices performance

#### 3.2.1. Accuracy assessment

This study applied both indices on Landsat OLI satellite images with different percentile thresholds to measure which threshold produces better results. A combination of NSAI1 T 85% OR NSAI2 T 92.5% shows the best result among the tested indices.

It is important to consider the aim of the study while using these indices. For soil mapping studies, a combination of A OR D provides the best overall ac-

Table 4. Accuracy assessment of proposed soil indices.

Instance	Index with threshold	User accuracy	Producers accuracy	Overall accuracy	Kappa coefficient	Commission error	Omission error
A	NSAI1 T 85%	0.690	0.723	0.900	0.646	0.310	0.277
B	NSAI1 T 87.5%	0.769	0.602	<b>0.904</b>	0.620	0.231	0.398
C	NSAI2 T 90%	0.750	0.542	0.894	0.569	0.250	0.458
D	NSAI2 T 92.5%	<b>0.867</b>	0.470	0.900	0.558	<b>0.133</b>	0.530
E	Combination of A OR C	0.646	<b>0.771</b>	0.892	0.638	0.354	<b>0.229</b>
F	Combination of A OR D	0.692	0.759	<b>0.904</b>	<b>0.666</b>	0.308	0.241

curacy and Kappa coefficient results. On the contrary, if the study intends to use it to refine urban ISA areas, indices with lower commission errors should be prioritized. NDSI2, with a 92.5% threshold provides the least commission error in this case.

### 3.2.2. Spectral difference index (SDI) value

SDI value above 1 refers to reasonable separation, and above 2 refer good separation.

Table 5. SDI of selected soil indices between soil and urban.

Index	SDI of Urban vs. Soil
MBSI	0.3101
BCI	0.4167
BI <sub>2002</sub>	0.7143
TC1	0.9269
DBSI	1.021
CI	1.0357
NDSI <sub>2010</sub>	1.3346
NDSI <sub>2015</sub>	1.5544
RNDSI	1.6358
NSAI2	1.8044
NSAI1	2.3204

## 4. Discussion

The proposed NSAI1 and NSAI2 indices have better separability of bare soil area and impervious surface area than previous indices, making it easier to extract bare soil area using a threshold. These indices also can be applied to

temporal studies using long collections of Landsat datasets and are compatible with temporal, fusion, and urban studies. This discussion section will further explore these novel indices' potential applications and implications in soil area enhancement and classification.

#### *4.1. Significance of the indices*

The proposed NSAI1 and NSAI2 are more effective in soil area enhancement using raw multispectral RS. These indices can be applied with imagery containing water bodies. Besides, both indices show bare soil area in the highest value, followed by ISA, vegetation and water bodies. These novel indices show significantly better soil and urban ISA separability from SDI results than previously developed indices. Combinedly, these indices can increase accuracy further. These indices used commonly available multispectral bands and are therefore applicable to temporal studies using a historical collection of multispectral datasets.

The significance of NSAI1 and NSAI2 is their separability of bare soil and impervious surface areas. Both indices have higher SDI values than other soil indices (Tab. 5). Therefore, extracting bare soil area using a threshold is easier without removing other LULC classes in pre-processing steps.

##### *4.1.1. Multispectral soil index*

Landsat multispectral imagery has been used for its popularity, free access, stable and long global archive. We wanted to utilize the spectral bands from Landsat to maintain replicability globally. In the literature review, we observed that  $NDSI_{2010}$  is a popular soil indices (Rogers and Kearney, 2010) which is also familiar as normalized difference of built-up index (NDBI) (Zha et al., 2003). We wanted to improve the index further to make it more sensitive to bare soil and less sensitive to the urban built-up area. This index uses SWIR1 and NIR bands.

Additionally,  $NDSI_{2015}$  uses SWIR2 and Green bands. We tried to compile these two soil indices to improve their soil sensitivity. But, we found that SWIR1 generalizes the soil area better than SWIR2 bands. SWIR1 bands differentiate bare soil and urban built-up area better than other bands. Therefore, we used only SWIR1 and did not use the SWIR2 band. Additionally, multiplication of Green and NIR bands make a good composite bands for soil indices. We also found that, Blue bands with SWIR amplify bare soil area and suppress vegetation and water areas. Therefore, we have used multiple versions of composite indices similar to NSAI1 and NSAI2. Only the proposed two indices have significant SDI values for bare soil and urban built-up area.

The benefit of multispectral soil indices is coverage availability and higher temporal resolution. A hyperspectral dataset may help better classify soil area from other LULCs, but does not have global coverage like Landsat or sentinel-2 datasets. Microwave or Radar imaging also has some strength in soil moisture

and subsurface soil condition mapping. Radar remote sensing is also sensible surface roughness. But, these imaging techniques cannot generalize soil area and distinguish soil from other LULC classes based on roughness and moisture.

#### *4.1.2. Temporal study compatibility*

These indices used commonly available multispectral bands. They are Blue, Green, NIR and SWIR1 spectral band regions. These bands are available in Landsat; therefore, temporal studies are more meaningful with these two proposed indices. We specifically avoid some useful but recently available spectral bands to maintain these characteristics, such as Panchromatic and Coastal spectral bands.

#### *4.1.3. Fusion study compatibility*

Popular multispectral optical sensors all have some common and compatible spectral bands. Our proposed soil indices used only those common bands to be compatible with other multispectral sensors. Especially, Sentinel-2/MSI, ASTER, MODIS TERRA and similar sensors. Fusing NSAI1 and NSAI2 from multiple multispectral datasets is also feasible.

#### *4.1.4. Urban study compatibility*

The proposed indices are compatible to use alongside urban studies. In urban optical classification, urban built-up areas are often mixed up with bare soil areas due to their spectral similarity. Our proposed indices have higher separability compared to other indices in distinguishing them. Therefore, urban studies can refine urban area classification using these novel soil area indices.

### *4.2. Comparing with previous soil indices*

The study found that eight indices, including two proposed indices, have an SDI value of more than one between soil area and urban ISA. To these eight indices, SDI values with soil and other LULC classes have been measured. It is found that NSAI1 has the highest SDI value, followed by NSAI2.

SDI value greater than 1 indicates reasonable separability among soil and urban areas. Compared to previous urban and soil area indices, NSAI1 and NSAI2 significantly increase the separability of urban and bare soil area classes (See Tab. 5). Also, the soil area enhancement is significantly improved. The results show how the sand has been used to fill the low-lying wetlands of eastern Dhaka.

BCI was significant in pursuing the efforts of extracting urban areas free from bare soil area. That required removing the water bodies pixels in the image pre-processing stage. Although, SDI shows BCI achieves mild separability in between urban and bare soil area classes. In contrast, NSAI1 and NSAI2 achieve better SDI values while applying on the image, including water pixels.

Additionally, higher accuracy in soil area extraction is possible using TCT bands, such as RNDSI (Deng et al., 2015). Though different sensors have differ-

ent TCT coefficients, most multispectral sensors' TCT coefficients have already developed. A similar study is possible with Ratio Index for Bright Soil (RIBS) (Qiu et al., 2017), which is also very similar to RNDSI. They both use normalized first TCT bands as the denominator. But, RIBS uses the normalized form of Normalized Difference Snow Index (NDSI<sub>2004</sub>) (Salomonson and Appel, 2004) instead of Normalized Difference Soil Index (NDSI<sub>2015</sub>) (Deng et al., 2015). RIBS has a higher SDI value than RNDSI, which is lower than NSAI1. The study also found that RIBS shows water bodies are the highest value and amplify widely. Though the authors claim that RIBS indexing does not require water bodies removal, experiments show otherwise. Furthermore, soil area and ISA shows in very low value which is difficult to separate with thresholds.

Most importantly, indices (BI<sub>2014</sub>, RNDSI, RIBS) used in normalized TC1 bands are susceptible to outliers. In practice, all the TCT bands have irregular minimum and maximum values. Therefore, it is wise to trim these bands with 1 or 2 percent from both ends before normalizing them. Figure 3 compares nine existing soil indices and two proposed novel indices.

### *4.3. Future research directions*

Hyperspectral remote sensing is useful for mapping detailed soil characteristics, as Gomez et al. (2012) demonstrated. Such as organic carbon (Gomez et al., 2008), heavy metals (Wang et al., 2018), nutrients (Song et al., 2018), salinization (El-Hamid et al., 2020), and moisture (Ge et al., 2019). But, there is a lack of spectral soil indices based on hyperspectral data. A short-wave infrared fine particle index (SWIR FI) is used for soil clay content indexing (Liu et al., 2018). Similar indices may develop for better LULC classification. Urban trends or prediction studies can increase accuracy using this soil indices by minimizing false urban ISA signature (Ahmad et al., 2023). Besides, fusion studies are also compatible with NSAI indices because of their simple band mathematics. Diverse data types can be incorporate with NSAI indices for fusion studies (Shao et al., 2021).

These two indices used the SWIR1 band, which is sensitive to wetness. Microwave remote sensing is better at measuring soil moisture content and related properties. Active microwave remote sensing and passive multispectral remote sensing have potential in soil related studies (Hasan et al., 2014; Periasamy and Shanmugam, 2017). SAR data can easily distinguish buildings and infrastructure from the background (Zhao et al., 2013). The problem would be to differentiate flat impervious surfaces, such as, roads, parking lots, and similar urban features. Hopefully, newer indices can utilize the microwave sensing of soil properties and permeability to distinguish bare soil from impervious surface areas. It may be possible to combine multispectral, hyperspectral and microwave remote sensing for better soil indexing like Lausch et al. (2019) try to do in addition to LiDAR (light detection and ranging) dataset.

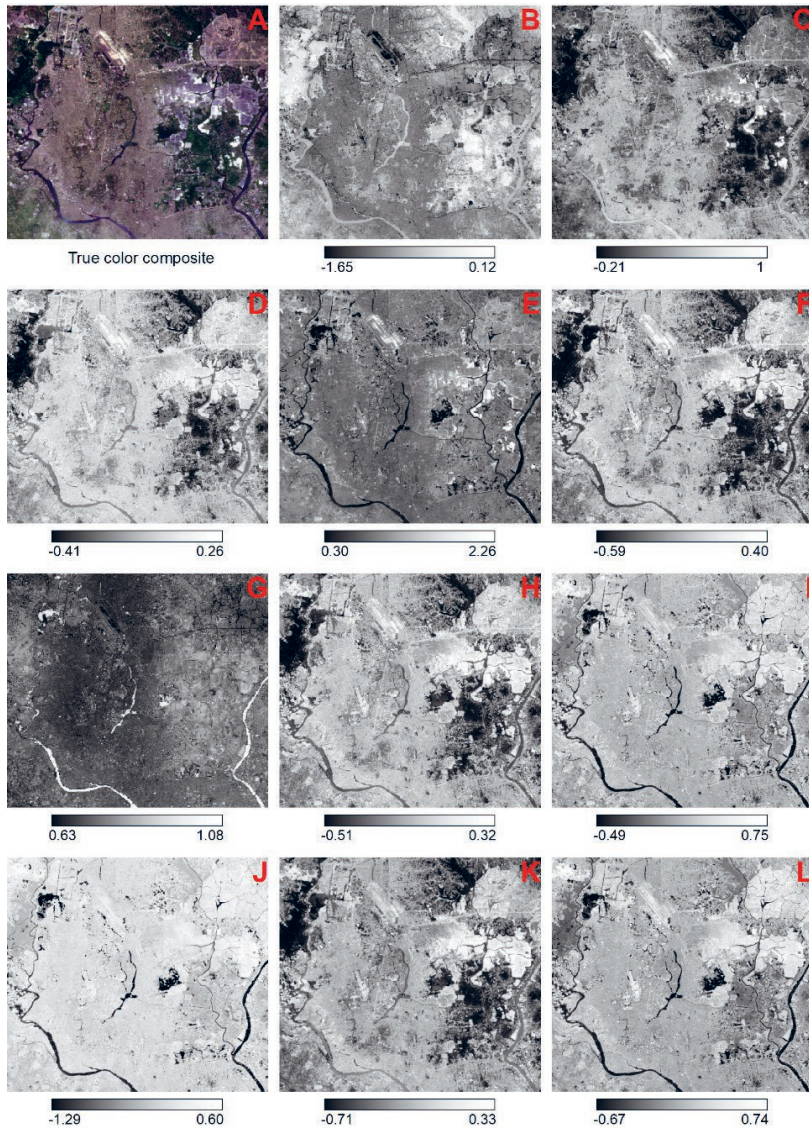


**Figure 3.** Soil Indices comparison: (A) RGB, (B) MBSI, (C) BCI, (D) BI<sub>2002</sub>, (E) TC1, (F) DBSI, (G) CI, (H) NDSI<sub>2010</sub>, (I) NDSI<sub>2015</sub>, (J) RNDSI, (K) NSAI<sub>2</sub>, (L) NSAI<sub>1</sub>.

Thresholding is also crucial if the study intends to classify soil areas. As the study shows, small changes in percentile threshold largely change the outcome value. This indexed value could easily be normalized into 0 to 1. After that, suitable thresholds can be tested against different regions with various soil conditions to determine better regional thresholds for these indices.

## 5. Conclusion

This study developed two novel soil indices that can automatically map soil areas from Landsat OLI imagery (30 m) on the GEE platform. NSAI1 and NSAI2 have SDI values, respectively, 2.32 and 1.80 for urban and soil areas. SDI values of developed indices are higher than all the comparing indices (Tab. 5). All of these indices have an overall accuracy of around 90%. Additionally, soil mapping revealed that a large part of the study area's eastern wetlands had been encroached (Fig. 2). These indices require no manual sample selection or removal of water bodies for soil area mapping. Therefore, these are free from human errors and map soil areas rapidly. Additionally, NSAI1 and NSAI2 indices are critical for refining urban ISA extraction results. Furthermore, regular and common multispectral bands made these two indices useful for temporal RS studies. Temporal studies included soil area-related studies, urban studies and so on.

*Acknowledgments* – This work was supported in part by the Guangxi science and technology program (GuiKe 2021AB30019); Sichuan Science and Technology Program (2022YFN0031, 2023YFN0022, and 2023YFS0381); Hubei key R & D plan (2022BAA048); Zhuhai industry university research cooperation project of China (ZH22017001210098PWC).

*Disclosure statement* – The authors declare no conflict of interest.

*Data availability statement* – The Landsat 8 dataset used in the study is freely accessible and Google Earth Engine (GEE) also help access is instantly. To access the dataset, use image collection id “LANDSAT/LC08/C01/T1\_RT” in GEE.

## References

- Ahmad, M. N., Shao, Z. and Javed, A. (2023): Modelling land use/land cover (LULC) change dynamics, future prospects, and its environmental impacts based on geospatial data models and remote sensing data, *Environ. Sci. Pollut. Res.*, **30**, 32985–33001, <https://doi.org/10.1007/s11356-022-24442-2>.
- As-syakur, A. R., Adnyana, I. W. S., Arthana, I. W. and Nuarsa, I. W. (2012): Enhanced built-up and bareness index (ebbi) for mapping built-up and bare land in an urban area, *Remote Sens.-Basel*, **4**, 2957–2970, <https://doi.org/10.3390/rs4102957>.
- Baghdadi, N., Choker, M., Zribi, M., Hajj, M. E., Paloscia, S., Verhoest, N. E., Lievens, H., Baup, F. and Mattia, F. (2016): A new empirical model for radar scattering from bare soil surfaces, *Remote Sens.-Basel*, **8**, 920, <https://doi.org/10.3390/rs8110920>.
- Baig, M. H. A., Zhang, L., Shuai, T. and Tong, Q. (2014): Derivation of a tasselled cap transformation based on landsat 8 at-satellite reflectance, *Remote Sens. Lett.*, **5**, 423–431, <https://doi.org/10.1080/02150704x.2014.915434>.
- Balenzano, A., Satalino, G., Lovergine, F., Rinaldi, M., Iacobellis, V., Mastronardi, N. and Mattia, F. (2013): On the use of temporal series of l- and x-band sar data for soil moisture retrieval. Capitanata plain case study, *Eur. J. Remote Sens.*, **46**, 721–737, <https://doi.org/10.5721/EuJRS20134643>.
- Bhatti, S. S. and Tripathi, N. K. (2014): Built-up area extraction using landsat 8 oli imagery, *GISci. Remote Sens.*, **51**, 445–467, <https://doi.org/10.1080/15481603.2014.939539>.

- Boisvert, J., Pultz, T., Brown, R. and Brisco, B. (1996): Potential of synthetic aperture radar for large-scale soil moisture monitoring: A review, *Can. J. Remote Sens.*, **22**, 2–13, <https://doi.org/10.1080/07038992.1996.10874632>.
- Chen, J., Zhang, M. Y., Wang, L., Shimazaki, H. and Tamura, M. (2005): A new index for mapping lichen-dominated biological soil crusts in desert areas, *Remote Sens. Environ.*, **96**, 165–175, <https://doi.org/10.1016/j.rse.2005.02.011>.
- Demattê, J. A., Huete, A. R., Ferreira, L. G., Nanni, M. R., Alves, M. C. and Fiorio, P. R. (2009): Methodology for bare soil detection and discrimination by landsat tm image, *Open Remote Sens. J.*, **2**, 24–35, <https://doi.org/10.2174/1875413901002010024>.
- Deng, C. and Wu, C. (2012): Bci: A biophysical composition index for remote sensing of urban environments, *Remote Sens. Environ.*, **127**, 247–259, <https://doi.org/10.1016/j.rse.2012.09.009>.
- Deng, Y., Wu, C., Li, M. and Chen, R. (2015): Rndsi: A ratio normalized difference soil index for remote sensing of urban/suburban environments. *Int. J. Appl. Earth Obs.*, **39**, 40–48, <https://doi.org/10.1016/j.jag.2015.02.010>.
- El-Hamid, A., Hazem, T. and Hong, G. (2020): Hyperspectral remote sensing for extraction of soil salinization in the northern region of Ningxia, *Model. Earth Syst. Environ.*, **6**, 2487–2493, <https://doi.org/10.1007/s40808-020-00829-3>.
- Ge, X., Wang, J., Ding, J., Cao, X., Zhang, Z., Liu, J. and Li, X. (2019): Combining uav-based hyperspectral imagery and machine learning algorithms for soil moisture content monitoring, *PeerJ*, **7**, e6926, <https://doi.org/10.7717/peerj.6926>.
- Ghulam, A., Qin, Q., Teyip, T. and Li, Z.-L. (2007): Modified perpendicular drought index (mpdi): A real-time drought monitoring method, *ISPRS J. Photogramm.*, **62**, 150–164, <https://doi.org/10.1016/j.isprsjprs.2007.03.002>.
- Ghulam, A., Qin, Q. and Zhan, Z. (2006): Designing of the perpendicular drought index, *Environ. Geol.*, **52**, 1045–1052, <https://doi.org/10.1007/s00254-006-0544-2>.
- Gomez, C., Lagacherie, P. and Coulouma, G. (2012): Regional predictions of eight common soil properties and their spatial structures from hyperspectral vis–nir data, *Geoderma*, **189**, 176–185, <https://doi.org/10.1016/j.geoderma.2012.05.023>.
- Gomez, C., Rossel, R. A. V. and McBratney, A. B. (2008): Soil organic carbon prediction by hyperspectral remote sensing and field vis-nir spectroscopy: An australian case study, *Geoderma*, **146**, 403–411, <https://doi.org/10.1016/j.geoderma.2008.06.011>.
- Hadria, R., Duchemin, B., Baup, F., Le Toan, T., Bouvet, A., Dedieu, G. and Le Page, M. (2009): Combined use of optical and radar satellite data for the detection of tillage and irrigation operations: Case study in central Morocco, *Agr. Water Manage.*, **96**, 1120–1127, <https://doi.org/10.1016/j.agwat.2009.02.010>.
- Hasan, S., Montzka, C., Rüdiger, C., Ali, M., Bogena, H. R. and Vereecken, H. (2014): Soil moisture retrieval from airborne l-band passive microwave using high resolution multispectral data, *ISPRS J. Photogramm.*, **91**, 59–71, <https://doi.org/10.1016/j.isprsjprs.2014.02.005>.
- Hua, L., Zhang, X., Chen, X., Yin, K. and Tang, L. (2017): A feature-based approach of decision tree classification to map time series urban land use and land cover with landsat 5 tm and landsat 8 oli in a coastal city, China, *ISPRS Int. J. Geo-Inf.*, **6**, 18, <https://doi.org/10.3390/ijgi6110331>.
- Huisman, J. A., Hubbard, S. S., Redman, J. D. and Annan, A. P. (2003): Measuring soil water content with ground penetrating radar: A review, *Vadose Zone J.*, **2**, 476–491, <https://doi.org/10.2136/vzj2003.4760>.
- Karnieli, A. (1997): Development and implementation of spectral crust index over dune sands, *Int. J. Remote Sens.*, **18**, 1207–1220, <https://doi.org/10.1080/014311697218368>.
- Kauth, R. J. and Thomas, G. S. (1976). The tasselled cap – a graphic description of the spectral-temporal development of agricultural crops as seen by landsat, in: *Symposium on Machine Processing of Remotely Sensed Data*. Purdue University, West Lafayette, Indiana: IEEE.

- Kawamura, M., Jayamanna, S. and Tsujiko, Y. (1997): Quantitative evaluation of urbanization in developing countries using satellite data, *Doboku Gakkai Ronbunshu*, **1997**, 45–54.
- Khaleda, S., Mowla, Q. A. and Murayama, Y. (2017): Dhaka metropolitan area, in: *Urban Development in Asia and Africa. The Urban Book Series*, edited by: Murayama, Y., Kamusoko, C., Yamashita, A. and Estoque, R. Springer, Singapore, 195–215, [https://doi.org/10.1007/978-981-10-3241-7\\_10](https://doi.org/10.1007/978-981-10-3241-7_10).
- Klotzsche, A., Jonard, F., Looms, M. C., van der Kruk, J. and Huisman, J. A. (2018): Measuring soil water content with ground penetrating radar: A decade of progress, *Vadose Zone Journal*, **17**, 1–9, <https://doi.org/10.2136/vzj2018.03.0052>.
- Lausch, A., Baade, J., Bannehr, L., Borg, E., Bumberger, J., Chabrilliat, S., Dietrich, P., Gerighausen, H., Glässer, C. and Hacker, J. M. (2019): Linking remote sensing and geodiversity and their traits relevant to biodiversity – part i: Soil characteristics, *Remote Sens.-Basel*, **11**, 2356, <https://doi.org/10.3390/rs11202356>.
- Li, H., Wang, C., Zhong, C., Su, A., Xiong, C., Wang, J. and Liu, J. (2017): Mapping urban bare land automatically from landsat imagery with a simple index, *Remote Sens.-Basel*, **9**, 249, <https://doi.org/10.3390/rs9030249>.
- Li, S. and Chen, X. (2014): A new bare-soil index for rapid mapping developing areas using landsat 8 data, *The International Archives of the Photogrammetry, Remote Sensing and Spatial Information Sciences*, **XL-4**, 139–144, <https://doi.org/10.5194/isprsarchives-XL-4-139-2014>.
- Li, Z. and Tan, D. (2013): The second modified perpendicular drought index (mpdi1): A combined drought monitoring method with soil moisture and vegetation index, *J. Indian Soc. Remote Sens.*, **41**, 873–881, <https://doi.org/10.1007/s12524-013-0264-5>.
- Liu, L., Ji, M. and Buchroithner, M. (2018): Transfer learning for soil spectroscopy based on convolutional neural networks and its application in soil clay content mapping using hyperspectral imagery, *Sensors*, **18**, 3169, <https://doi.org/10.3390/s18093169>.
- Liu, X., Chen, J., Cui, X., Liu, Q., Cao, X. and Chen, X. (2019): Measurement of soil water content using ground-penetrating radar: A review of current methods, *Int. J. Digit. Earth*, **12**, 95–118, <https://doi.org/10.1080/17538947.2017.1412520>.
- McNairn, H. and Brisco, B. (2004): The application of c-band polarimetric sar for agriculture: A review, *Can. J. Remote Sens.*, **30**, 525–542, <https://doi.org/10.5589/m03-069>.
- Mishra, A. K. and Singh, V. P. (2010): A review of drought concepts, *J. Hydrol.*, **391**, 202–216, <https://doi.org/10.1016/j.jhydrol.2010.07.012>.
- Periasamy, S. and Shanmugam, R. S. (2017): Multispectral and microwave remote sensing models to survey soil moisture and salinity, *Land Degrad. Dev.*, **28**, 1412–1425, <https://doi.org/10.1002/ldr.2661>.
- Piyooosh, A. K. and Ghosh, S. K. (2017): Development of a modified bare soil and urban index for landsat 8 satellite data, *Geocarto Int.*, **33**, 423–442, <https://doi.org/10.1080/10106049.2016.1273401>.
- Prevot, L., Champion, I. and Guyot, G. (1993): Estimating surface soil moisture and leaf area index of a wheat canopy using a dual-frequency (c and x bands) scatterometer, *Remote Sens. Environ.*, **46**, 331–339, [https://doi.org/10.1016/0034-4257\(93\)90053-Z](https://doi.org/10.1016/0034-4257(93)90053-Z).
- Qiu, B., Zhang, K., Tang, Z., Chen, C. and Wang, Z. (2017): Developing soil indices based on brightness, darkness, and greenness to improve land surface mapping accuracy, *Gisci. Remote Sens.*, **54**, 759–777, <https://doi.org/10.1080/15481603.2017.1328758>.
- Radeloff, V. C., Mladenoff, D. J. and Boyce, M. S. (1999): Detecting jack pine budworm defoliation using spectral mixture analysis: Separating effects from determinants, *Remote Sens. Environ.*, **69**, 156–169, [https://doi.org/10.1016/S0034-4257\(99\)00008-5](https://doi.org/10.1016/S0034-4257(99)00008-5).
- Rasul, A., Balzter, H., Ibrahim, G., Hameed, H., Wheeler, J., Adamu, B., Ibrahim, S. a. and Najmaddin, P. (2018): Applying built-up and bare-soil indices from landsat 8 to cities in dry climates, *Land*, **7**, <https://doi.org/10.3390/land7030081>.

- Rikimaru, A., Roy, P. and Miyatake, S. (2002): Tropical forest cover density mapping, *Trop. Ecol.*, **43**, 39–47.
- Rogers, A. S. and Kearney, M. S. (2010): Reducing signature variability in unmixing coastal marsh thematic mapper scenes using spectral indices, *Int. J. Remote Sens.*, **25**, 2317–2335, <https://doi.org/10.1080/01431160310001618103>.
- Salomonson, V. V. and Appel, I. (2004): Estimating fractional snow cover from modis using the normalized difference snow index, *Remote Sen. Environ.*, **89**, 351–360, <https://doi.org/10.1016/j.rse.2003.10.016>.
- Shao, Z., Sumari, N. S., Portnov, A., Ujoh, F., Musakwa, W. and Mandela, P. J. (2021) Urban sprawl and its impact on sustainable urban development: A combination of remote sensing and social media data, *Geo-Spat. Inf. Sci.*, **24**(2), 241–255, <https://doi.org/10.1080/10095020.2020.1787800>.
- Song, Y.-Q., Zhao, X., Su, H.-Y., Li, B., Hu, Y.-M. and Cui, X.-S. (2018): Predicting spatial variations in soil nutrients with hyperspectral remote sensing at regional scale, *Sensors*, **18**, 3086, <https://doi.org/10.3390/s18093086>.
- Srivastava, S. and Mishra, G. (2004): Study of the characteristics of the soil of chhattisgarh at x-band frequency, *Sadhana*, **29**, 343–347, <https://doi.org/10.1007/BF02703685>.
- Taconet, O., Benallegue, M., Vidal-Madjar, D., Prevot, L., Dechambre, M. and Normand, M. (1994): Estimation of soil and crop parameters for wheat from airborne radar backscattering data in C and X bands, *Remote Sens. Environ.*, **50**, 287–294, [https://doi.org/10.1016/0034-4257\(94\)90078-7](https://doi.org/10.1016/0034-4257(94)90078-7).
- Wang, F., Gao, J. and Zha, Y. (2018): Hyperspectral sensing of heavy metals in soil and vegetation: Feasibility and challenges, *ISPRS J. Photogramm.*, **136**, 73–84, <https://doi.org/10.1016/j.isprsjprs.2017.12.003>.
- Waqar, M. M., Mirza, J. F., Mumtaz, R. and Hussain, E. (2012): Development of new indices for extraction of built-up area and bare soil from landsat data, *Open Access Scientific Reports*, **1**, 4, <https://doi.org/10.4172/scientificreports.136>.
- Yamane, Y., Kiguchi, M., Terao, T., Murata, F. and Hayashi, T. (2014): Climatic variability, *Dhaka Megacity* (pp. 61–73): Springer.
- Zajícová, K. and Chuman, T. (2019): Application of ground penetrating radar methods in soil studies: A review, *Geoderma*, **343**, 116–129, <https://doi.org/10.1016/j.geoderma.2019.02.024>.
- Zha, Y., Gao, J. and Ni, S. (2003): Use of normalized difference built-up index in automatically mapping urban areas from tm imagery, *Int. J. Remote Sens.*, **24**, 583–594, <https://doi.org/10.1080/01431160304987>.
- Zhang, S., Yang, K., Li, M., Ma, Y. and Sun, M. (2018): Combinational biophysical composition index (cbci) for effective mapping biophysical composition in urban areas, *IEEE Access*, **6**, 41224–41237, <https://doi.org/10.1109/ACCESS.2018.2857405>.
- Zhao, H. and Chen, X. (2005): Use of normalized difference bareness index in quickly mapping bare areas from tm/etm+, in: *International Geoscience and Remote Sensing Symposium* (p. 1666).
- Zhao, H., Chen, X., Zhang, Z. and Zhou, Y. (2019): Exploring an efficient sandy barren index for rapid mapping of sandy barren land from landsat tm/oli images, *Int. J. Appl. Earth Obs.*, **80**, 38–46, <https://doi.org/10.1016/j.jag.2019.04.001>.
- Zhao, L., Zhou, X. and Kuang, G. (2013): Building detection from urban sar image using building characteristics and contextual information, *Eurasip J. Adv. Sig. Pr.*, **2013**, 1–16, <https://doi.org/10.1186/1687-6180-2013-56>.

## SAŽETAK

**Razvoj normaliziranog indeksa tla za urbane studije upotrebom podataka daljinskih mjerenja**

*Akib Javed, Zhenfeng Shao, Bin Bai, Zhuoyang Yu, Jiabing Wang, Iffat Ara, Md. Enamul Huq, Md. Yeamin Ali, Nayyer Saleem, Muhammad Nasar Ahmad, Neema Simon Sumari i Mardia*

Ovaj rad prikazuje dva nova spektralna indeksa tla kako bi se identificiralo golo tlo te kako bi se bolje razlikovalo od urbanih nepropusnih površina (ISA). Ti indeksi su definirani na temelju srednje prostorne rezolucije daljinskih podataka Landsat 8 OLI skupa podataka. U multispektralnim daljinskim mjerenjima (RS) prepoznavanje golog tla ili urbane ISA podloge je složenije od prepoznavanja vodenih tijela ili podloge s vegetacijom. Zbog sličnosti spektara dobivenih multispektralnim senzorima golo tlo i urbana ISA površina često se ne razlučuju. Ova studija predlaže dva normalizirana indeksa tla (NSAI1 i NSAI2) korištenjem tipičnih multispektralnih pojaseva. Eksperimenti pokazuju da ta dva indeksa imaju sveukupnu točnost od približno 90%. Indeks spektralne sličnosti (SDI) pokazuje da ta dva indeksa razlikuju golo tlo od urbane ISA podloge bolje nego dosadašnji indeksi. Rezultati pokazuju da percentilni pragovi mogu efikasno razlučiti površine s golim tlom od pozadine. Kombiniranom upotrebom oba indeksa izmjerena je površina tla veća od 71 km<sup>2</sup>. Najznačajniji rezultat je taj da predloženi indeksi tla mogu poboljšati točnost mjerenja urbanih ISA u u prostorno-vremenskim studijama.

*Ključne riječi:* indeks tla, NSAI1, NSAI2, LULCC, Dhaka

*Corresponding author's address:* Akib Javed, State Key Laboratory of Information Engineering in Surveying, Mapping and Remote Sensing, Wuhan University, Wuhan, Hubei 430079, China; e-mail: akibjaved@whu.edu.cn



This work is licensed under a Creative Commons Attribution-NonCommercial 4.0 International License.